View Article Online / Journal Homepage / Table of Contents for this issue
Dynamic Article Links
Soft Matter
Cite this: *Soft Matter*, 2011, **7**, 7003
www.rsc.org/softmatter

PAPER

Effects of the interaction and surface morphology of mixed DPoPE/ Poloxamer 188 monolayers and thin liquid films

Albena Jordanova,[a] Boris Tenchov[ab] and Zdravko Lalchev*[c]

Received 31st January 2011, Accepted 4th May 2011
DOI: 10.1039/c1sm05165b

The aim of the present study is to investigate the kinetics and the penetration degree of Poloxamer 188 (P188) of different concentrations to Langmuir lipid monolayers at the air–water interface formed from dipalmitoleoylphosphatidylethanolamine (DPoPE) in different liquid crystalline phase states, lamellar L_α and non-lamellar (inverse hexagonal H_{II} and inverse bicontinuous cubic Q_{II}) phases, in static and dynamic conditions. It was found that the penetration of P188 to the DPoPE monolayers in all three lipid phases is very fast, strong and concentration dependent, and the strongest effect was detected for the non-lamellar DPoPE monolayers. Moreover, the dynamic characteristics of the mixed DPoPE + P188 monolayers revealed stronger interactions between P188 and DPoPE in Q_{II} phase, than in the other two, and more packed surface structures. In addition, by using Brewster angle microscopy (BAM), the surface morphology of mixed DPoPE + P188 monolayers was determined. The BAM images showed that the addition of P188 to DPoPE monolayers led to decrease in the lipid domain size and to formation of more homogeneous films. Furthermore, the effects of P188 on the hydrodynamic properties and the stability of lipid thin liquid films (LTLFs) were studied. A strong stabilization effect of P188 to the LTLF films was proved. This effect was probably influenced by the appearance of steric repulsion (in addition to the electrostatic repulsion and van der Waals attractive forces). The results suggested that the non-lamellar lipid phases have higher potential to act as a "reservoir" for penetrating agents, and as a pool for membrane repairing substances such as P188.

1. Introduction

Lipid–water dispersions are able to self-organize into different geometrical structures including lamellar and non-lamellar phases,[1–3] and the membrane lipids may form different kinds of monolayers of physiological significance at the air–water interface.[4] The phosphatidylethanolamines (PEs) are a major lipid class in the cell membranes that could form both lamellar and non-lamellar structures under physiological conditions.[5–7] In the cell the PEs are predominately in a bilayer, fluid lamellar (L_α) state. The role of the non-lamellar PEs phases—the inverse hexagonal H_{II} and the inverse bicontinuous cubic Q_{II} phases—has been subject of many investigations. The non-lamellar lipid phases are characterized by a curvature of their component in the lipid structures where the molecules are assembled not into bilayers but into cylinders (H_{II}) and cubes (Q_{II}). These non-lamellar phases take part in some important cell processes such as membrane fusion;[2,8] cell division;[9] cell signal transduction;[6,10] transmembrane transport of ions and large molecules,[11] *etc.*

The poloxamers are a class of water soluble non-ionic multiblock copolymers that have important surface-active properties and could interact with membrane lipids. The poloxamer series covers a range of liquids, pastes and solids, with molecular weights varying from 1100 Da to about 14000 Da. It is demonstrated that the poloxamers are effective in sealing permeabilized cell membranes: against loss of carboxy-fluorescein dye after electroporation;[12,13] membrane pores in skeletal muscle cells after electrical injuries; heat shocks; thermal burns; frostbite; radiation and ischemia-reperfusion injuries[13–16] *etc.*, that lead to cell membrane structural integrity loss. The possibility to repair cell membrane wounds using synthetic surfactants is now well established but the exact mechanism of sealing is still under investigation.

The noncytotoxic biosurfactant Poloxamer 188 (P188) is a three-block copolymer (hydrophilic polyethylene oxide, PEO, hydrophobic polypropylene oxide, PPO, hydrophilic polyethylene oxide, PEO) with amphiphillic structure which is known to repair damaged membranes and thus to restore the structural integrity and function of the cells both *in vitro* and *in vivo*.[17–23] P188 has a molecular weight of about 8400 Da and its hydrophilic part is about 80% of the total molecular weight. The PEO

[a]*Institute of Biophysics and Biomedical Engineering, Bulgarian Academy of Sciences, 21 Georgi Bonchev blvd., 1113 Sofia, Bulgaria*
[b]*Ohio State University College of Pharmacy, Parks Hall, Columbus, OH, 43210, USA*
[c]*Department of Biochemistry, Faculty of Biology, St. Kliment Ohridski University of Sofia, 8 Dragan Tsankov str., 1164 Sofia, Bulgaria. E-mail: lalchev@biofac.uni-sofia.bg*

chains (each including 76 monomer units) are hydrophillic due to their short carbon units between the oxygen bridges whereas the PPO center (formed from 29 monomers) is hydrophobic due to the larger propylene unit. P188 was the first copolymer tested for membrane recovery widely used in medicine, pharmacy and cosmetic industry as a solubilizing, wetting and emulsifying agent with low toxicity and high solubility. It is proven that P188 can seal membrane pores in skeletal muscle cells after heat shock,[24] enhance the functional recovery of lethally heat-shocked fibroblasts,[25] and damages after high dose ionizing radiation.[26] Moreover, it is shown that P188 can repair damages to cardiac muscle cell membrane;[27] effectively restores, protects fat grafts, and improves cell survival *via* decreased fat graft apoptosis;[28] has neuroprotection against a broad range of clinically relevant neural insults;[29] supports the delivery of drug nanoparticles into the brain[30] and is being used in breast cancer therapy to overcome multidrug resistance of tumor cells.[31]

We assume that the non-lamellar lipid phases, possessing different geometry, are an appropriate model for the investigation of the interaction between P188 and local damages in the biomembranes. It is known that the damaged membranes have higher surface tension in comparison to the normal biomembranes. Our previous results are in accordance with the literature data that P188 can penetrate into lipid monolayers when the surface tension is above 50 mN m^{-1}.[17,19,32] At lower surface tension the poloxamers can be "squeezed out" from the lipid bilayer of the biomembrane,[33] thus recovering its structural integrity. Moreover, we previously demonstrated that the DPoPE lipid structures of different geometry are able to disintegrate at the air–water interface to a different extent and that in comparison to the non-lamellar structures the L_α phase showed higher molecular repulsion in the plane of the monolayer during monolayer compression and much better molecular re-spreading during decompression.[33–35]

In addition, lipid thin liquid films (LTLFs) has been successfully used as an appropriate model system for molecular interactions between phospholipids and membrane-active agents, like dextrane sulfates, free PEGs and phospholipid linked PEGs at the air–water interfaces.[4,36–38] LTLFs are also a useful model of cell fusion processes,[39] the physiology of lung surfactant,[40–44] *etc.* The LTLFs consist of two lipid monolayers at the air–water interface, which contact each other through their polar head groups. It is shown that the use of both model systems (lipid monolayers and LTLFs) is very effective for studying the interactions at interfaces of membrane lipids in a different phase state with membrane-active agents from the bulk.[4,34,36–39,45–47]

The aim of the present study is to investigate the kinetics and penetration degree of P188 to the DPoPE monolayers of different liquid crystalline phase states, lamellar L_α and non-lamellar (H_{II} and Q_{II}), and to observe the surface morphology of the mixed DPoPE + P188 films. Another goal is to determine the differences in the dynamic characteristics of mixed DPoPE + poloxamer monolayers in different lipid phase states and P188 concentrations, during compression/decompression. Moreover, by using BAM and LTLFs the effects of P188 on the DPoPE film morphology, hydrodynamic properties and stability were studied. Our motivation was to attempt to clarify the molecular mechanisms of the interactions between P188 molecules and damaged cell membranes.

2. Experimental

Materials

1, 2-Dipalmitoleoyl-sn-*glycero*-3-phosphoethanolamine (DPoPE) was purchased from Avanti Polar Lipids (Alabaster, USA) and Poloxamer 188 was purchased from Anatrace (USA). By performing thin layer chromatography the purity of the DPoPE was checked. All solutions were made with deionized water with conductivity less than 1 μS cm^{-1}. (Crystal 5, Adrona Laboratory Systems, Latvia).

Surface tension measurements

Lipid dispersions of L_α and H_{II} phases were prepared by mechanical agitation in 0.5 M NaCl (Merck) solutions at different temperatures.[34] This DPoPE dispersions display $L_\alpha \rightarrow H_{II}$ transition at 39 °C during heating and this transition is reversible with a hysteresis of *ca.* 15 °C during cooling. Considering the above-mentioned hysterisis we accepted that the dispersions of DPoPE in 0.5 M NaCl at 37 °C after the first heating–cooling cycle are in H_{II} phase. An inverse bicontinuous cubic phase, Q_{II} of *Pn*3*m* (Q^{224}) type of DPoPE, was prepared by temperature cycling between 0 and 60 °C of the latter dispersion, as previously described.[48] After the preparation of the three lipid phases, they remain stable at 22 °C and at 37 °C as well, at which the experiments were conducted.

The monolayers of DPoPE in different phases (L_α, H_{II} and Q_{II}) were formed by spreading the DPoPE dispersion on a subphase of 0.5 M NaCl in a Langmuir trough with area of 1710 mm^2. The surface tension γ (mN m^{-1}) was followed with time by the Wilhelmy plate method,[34] using an automatic Wilhelmy tensiometer (Biegler Electronic, Austria). The trough was provided with a thermostat and the temperature in all experiments was 37 ± 0.5 °C. The amount of DPoPE dispersions was calculated to a definite surface concentration of 100 Å^2 per lipid molecule and γ decrease was detected until reaching an equilibrium value (γ_{eq}). After reaching γ_{eq} definite amounts of Poloxamer 188 (MW = 8400 Da) dissolved in 0.5 M NaCl solution were injected into the subphase at the bottom of the through. The amounts of P188 injected were calculated to correspond to a final P188 volume concentration of 1 μg ml^{-1} (low P188 concentration), 10 μg ml^{-1} (middle P188 concentration) and 20 μg ml^{-1} (high P188 concentration). The decrease in surface tension with time after the injection of P188, due to P188 adsorption and interaction with DPoPE at the interface, was detected until reaching the equilibrium values of γ.

By measuring the surface tension during compression/decompression between 100% (γ_{max}) and 20% (γ_{min}) of the initial monolayer area the dynamic characteristics of pure (DPoPE) and mixed (DPoPE + P188) monolayers were studied. The compression/decompression rate was 3 min per cycle. The monolayer surface tension was monitored up to the 3th cycle.

Experimental errors are ± 0.5 mN m^{-1} for the surface tension of three different measurements.

Brewster angle microscopy of monolayers

Brewster angle microscopy (BAM) provided a well-suited approach for visualization of the lateral domains formation in monolayers without fluorescent probes.[49,50] Insoluble DPoPE monolayers (in absence or presence of P188) at the air–water interface of Langmuir trough were formed by spreading the phospholipid molecules dissolved in chloroform over the subphase of 0.15 M NaCl. At least 20 min were provided for chloroform evaporation. At surface lipid concentration of 20 Å^2 mol^{-1} the monolayer morphology changes after the addition of P188 into the subphase were monitored and BAM images with dimensions 3600 × 4000 μm using Micro BAM2 (Nima Technology Ltd, Coventry, UK) equipped with laser diode (659 nm, 30 mW at laser aperture) were recorded. The temperature of the subphase was controlled to be 22 ± 0.5 °C. The polarizer and analyzer were set to p-polarization and the incoming laser light was limited to an angle of incidence of 53 ± 2° (Brewster angle for water or aqueous solutions). The images obtained were analyzed and processed using the integrated software.

Formation of lipid thin liquid films (LTLFs)

LTLFs were investigated by the microinterferometric method of Scheludko and Exerowa[51,52] using a modified measuring cell by Lalchev *et al.*[4] In a specially constructed glass cell microscopic horizontal DPoPE films with a radius of 0.22 mm were formed in the middle of a biconcave drop. The glass cell was equipped with an optical system for observation and investigation of LTLFs (microscope for reflected light). The lipid solution volume in the glass cell was 70 μl and the DPoPE concentrations were varied from 20 to 60 μg ml^{-1}. Different electrolyte concentrations, from 0.001 M NaCl to 0.5 M NaCl, were used. Before film formation at least 30 min were given the LTLFs for reaching equilibrium phospholipid adsorption to the monolayers, for vapour pressure saturation in the glass cell and for temperature adjustment. The measuring cell was thermostatted at 22 °C with an accuracy within ± 0.1 °C. After sucking the solution from the biconcave drop, thick LTLF was formed, as previously described.[36,52] Further, the film spontaneously became thinner, changing its color from yellow to gray and dark-gray with decreasing its thickness, respectively. After a characteristic film thinning time, t_1 (sec), a critical film thickness was reached (*ca.* 300 Å). Then a black spot (BS), a local thinning in the film, expanded to fill up the whole area of the film and at different experimental conditions two types of stable black films could be formed: common black films, CBFs and Newton black films, NBFs.[42,52] CBF contains a free water layer between the two monolayers with thickness ranging from 10 to 25 nm, while NBF contains no free water and its thickness is less than 8 nm. The formation of both stable CBF and NBF is possible only at lipid concentration above the threshold concentration C_t, since bellow C_t the films always rupture, *i.e.* the films are in unstable state. The kinetics of the film formation was detected by measuring the film thinning time (t_1) and the film lifetime (τ). The film lifetime represented the time of its formation to its rupture. It is considered that the films with a lifetime of more than 15 min are stable films. The LTLFs photographs were made by a digital camera Olympus (C-7070) connected to an inverted light microscope (Carl Zeiss Jena) with an optical adaptor (C3040-ADU) provided by the manufacturer. The LTLFs images were captured in the camera's manual mode in equal conditions (camera speed, microscope illumination *etc.*).

Determination the effects of the addition of Poloxamer 188 to DPoPE films

8 μl Poloxamer 188 (with concentration 0.84 mg ml^{-1}, 1 × 10^{-4} M) was added dropwise to 70 μl DPoPE solutions of 0.001 M NaCl to 0.1 M NaCl (with lipid concentration from 20 to 60 μg ml^{-1}). The final volume concentration of P188 was 86 μg ml^{-1} (10 μM). The concentrations of the pure DPoPE films were chosen to be bellow C_t needed for stable DPoPE films formation. At this concentration films always rupture and thus we studied the effects of P188 on unstable lipid films. The effects of Poloxamer 188 were tested by measuring the film thinning time (t_1), the film type and color and the film lifetime (τ). At least 10 measurements were made at each sample preparation.

3. Results and discussion

Spreading kinetics of DPoPE and penetration of P188 to the lipid monolayers

The surface behavior of the three different DPoPE phases spread at the air–water interface at a surface concentration corresponding to 100 Å^2 per lipid molecule was studied. The surface tension–time (γ/t) curves for the three liquid crystalline lipid phases recorded at 37 °C showed that γ decreased rapidly to the equilibrium value (γ_{eq}). The best spreading observed was for the lamellar L_α phase (Fig. 1), followed by the cubic Q_{II} (Fig. 2) and H_{II} phase (Fig. 3). At this surface concentration γ decreased to 64.2 mN m^{-1} for the L_α phase, to 67.3 mN m^{-1} for the Q_{II} phase, and to 68.6 mN m^{-1} for the H_{II} phase respectively (Fig. 1–3).

The monolayers formed by the adsorption of pure P188 to the air–water interface with a volume concentration of 1 μg ml^{-1} (low P188 concentration) reduced the surface tension from 72.9 to

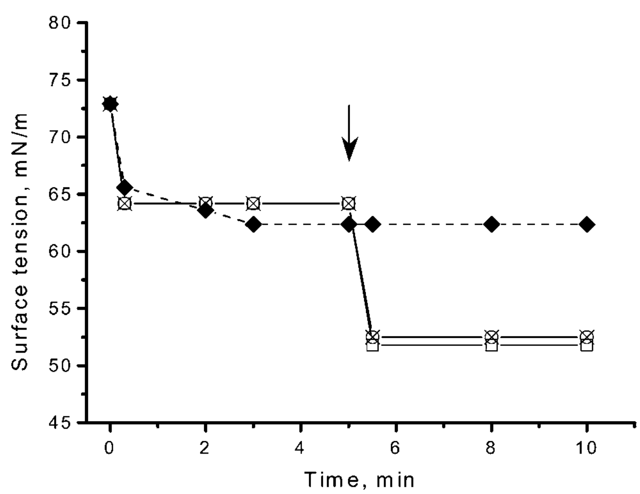

Fig. 1 Surface tension (γ, mN m^{-1}) as a function of time (min) for spread monolayers of DPoPE lamellar L_α phase on 0.5 M NaCl subphase at 37 °C. The arrow points at the addition of P188 dispersion into the subphase. The dotted line shows the reduction of the surface tension by adsorption of pure P188 with a high volume concentration of 20 μg ml^{-1}. The symbols denote: (○) – 100 Å^2/phospholipid molecule + low P188 concentration (1 μg ml^{-1}); (×) – 100 Å^2/phospholipid molecule + middle P188 concentration (10 μg ml^{-1}); (□) - 100 Å^2/phospholipid molecule + high P188 concentration (20 μg ml^{-1}).

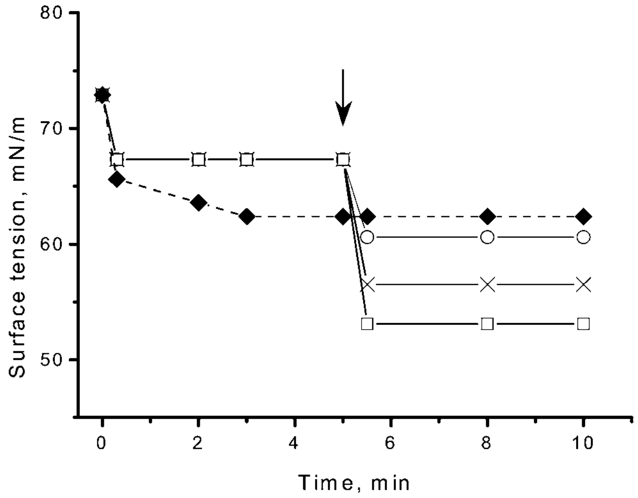

Fig. 2 Surface tension (γ, mN m^{-1}) as a function of time (min) for spread monolayers of DPoPE inverse bicontinuous cubic Q_{II} phase on 0.5 M NaCl solution at 37 °C. The arrow points at the addition of P188 dispersion into the subphase. The dotted line shows reduction of the surface tension by adsorption of pure P188 with a high volume concentration of 20 μg ml^{-1}. The symbols denote: (○) – 100 Å^2/phospholipid molecule + low P188 concentration (1 μg ml^{-1}); (×) – 100 Å^2/phospholipid molecule + middle P188 concentration (10 μg ml^{-1}); (□) - 100 Å^2/phospholipid molecule + high P188 concentration (20 μg ml^{-1}).

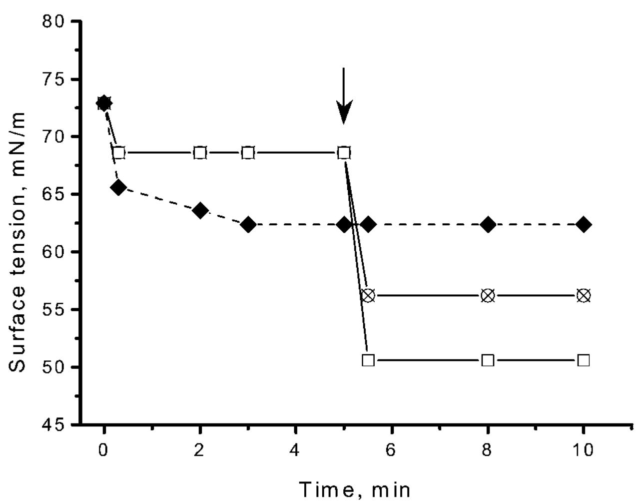

Fig. 3 Surface tension (γ, mN m^{-1}) as a function of time (min) for spread monolayers of DPoPE inverse hexagonal H_{II} phase on 0.5 M NaCl solution at 37 °C. The arrow points at the addition of P188 dispersion into the subphase. The dotted line shows reduction of surface tension by adsorption of pure P188 with a high volume concentration of 20 μg ml^{-1}. The symbols denote: (○) – 100 Å^2/phospholipid molecule + low P188 concentration (1 μg ml^{-1}); (×) – 100 Å^2/phospholipid molecule + middle P188 concentration (10 μg ml^{-1}); (□) – 100 Å^2/phospholipid molecule + high P188 concentration (20 μg ml^{-1}).

65.6 mN m^{-1} ($\Delta\gamma$ = 7.3 mN m^{-1}), and with a volume concentration of 20 μg ml^{-1} (high P188 concentration, being below its critical micelle concentration, CMC = 1.25 × 10^{-4} M) reduced γ to 62.4 mN m^{-1}, (Table 1). Our results demonstrated that P188 displayed high surface activity and adsorption to the air–water interface and reached a decrease in the surface tension of $\Delta\gamma$ = 10.5 mN m^{-1} at the highest concentration studied.

The penetration effect of the Poloxamer 188 injected into the subphase of the DPoPE monolayers showed that the P188 insertion is very strong and concentration dependent (Fig. 1–3). In all cases the penetration of P188 and the formation of DPoPE + P188 mixed monolayers was fast and the equilibrium values of the mixed monolayers was reached within 20–30 s. The data summarized in Table 2 revealed that the insertion of P188 molecules of low concentration was stronger to the DPoPE monolayers of L_α and H_{II} phases ($\Delta\gamma$ = 12.4 mN m^{-1} for both phases) in comparison to the Q_{II} phase ($\Delta\gamma$ = 6.7 mN m^{-1}). However, at concentration of 20 μg ml^{-1} the strongest penetration was detected to the H_{II} DPoPE monolayers ($\Delta\gamma$ = 18.0 mN m^{-1}), followed by Q_{II} ($\Delta\gamma$ = 14.2 mN m^{-1}), and L_α ($\Delta\gamma$ = 11.7 mN m^{-1}) phases. Thus regarding the insertion of high concentration of P188 molecules to monolayers of different phases the order $H_{II} > Q_{II} > L_\alpha$ was observed. The results showed that the increase in P188 concentration practically did not change the γ_{eq} value of the mixed poloxamer + L_α monolayer (even slightly increased it from 51.8 to 52.5 mN m^{-1}). In the same concentration range the γ_{eq} values (after the addition of P188 to the non-lamellar phases) decreased significantly, from 60.6 to 53.1 mN m^{-1} for P188 + Q_{II} and from 56.2 to 50.6 mN m^{-1} for P188 + H_{II} (Table 2). Based on the results obtained we could conclude that the increase in P188 concentration affected the penetration ability to the monolayers of the different lipid phase states in a different way. At low P188 concentration the poloxamer penetrated easily in to H_{II} and L_α phases predominantly, while at high bulk P188 concentration the penetration was easier to the non-lamellar phases but not to L_α phase. Thus at equal surface concentration these partially disintegrated H_{II} and Q_{II} phases provide more "free area" for the insertion of the surface-active agent P188. Hence, one can speculate that the non-lamellar H_{II} and Q_{II} phases could serve as a "surface reservoir" of bulk agents (like P188) at very high concentration (Table 2), and consequently, as a pool for membrane repairing substances. In addition, according to the literature data P188 penetrates into dipalmitoylphosphatidylcholine and dipalmitoylphosphatidylglycerol monolayers only at surface tension equal to and higher than 50 mN m^{-1}, but not at lower γ.[17,19,32] Our results confirm these observations for the monolayers of the three DPoPE phases studied.

Dynamic characteristics of mixed DPoPE + P188 monolayers

In our study two types of tensiometric experiments with DPoPE films (pure or in the presence of P188) were performed: (i) registration of the kinetics of the surface tension decrease until reaching the equilibrium value (γ_{eq}), and (ii) measurement of the dynamic (at interfacial compression/decompression) surface tension characteristics, γ_{max} and γ_{min}. The minimal surface tension (γ_{min}) realized at the final stage of interfacial compression depends on the maximal surface packing density. The maximal surface tension (γ_{max}) observed after interfacial expansion reflects the degree of surface readsorption and rearrangement of the film.

The γ values for pure P188 obtained during compression/decompression cycles showed that γ_{max} values increased from

Table 1 Equilibrium values of the surface tension, γ_{eq} (mN m^{-1}), of pure P188 adsorption monolayers at different volume concentrations into the subphase of 0.5 M NaCl at 37 °C. The experimental errors are ± 0.5 mN m^{-1} for the surface tension from three different measurements

Concentration of P188 (μg ml^{-1})	Concentration of P188 (μM)	γ equilibrium, (mN m^{-1})	$\Delta\gamma$ (mN m^{-1}) ($\Delta\gamma = \gamma_{H2O}$-$\gamma_{eq}$)
1	0.119	65.6	7.3
10	1.19	63.4	9.5
20	2.38	62.4	10.5

Table 2 Equilibrium values of the surface tension, γ_{eq} (mN m^{-1}), of pure DPoPE monolayers and mixed DPoPE + P188 monolayers. The experimental errors are ± 0.5 mN m^{-1} for surface tension from three different measurements

	γ_{eq}; L_α phase	γ_{eq}; Q_{II} phase	γ_{eq}; H_{II} phase
DPoPE (100 Å^2 mol^{-1})	64.2	67.3	68.6
DPoPE+ low P188 concentration	51.8 $\Delta\gamma$ = 12.4	60.6 $\Delta\gamma$ = 6.7	56.2 $\Delta\gamma$ = 12.4
DPoPE+middle P188 concentration	52.5 $\Delta\gamma$ = 11.7	56.5 $\Delta\gamma$ = 10.8	56.2 $\Delta\gamma$ = 12.4
DPoPE+ high P188 concentration	52.5 $\Delta\gamma$ = 11.7	53.1 $\Delta\gamma$ = 14.2	50.6 $\Delta\gamma$ = 18.0

62.4 mN m^{-1} in the first cycle to 65.8 mN m^{-1} in the 3th cycle. The corresponding values of γ_{min} were 42.1 mN m^{-1} in the first and 40.6 mN m^{-1} in the 3th cycle, *i.e.* in contrast to γ_{max}, the values of γ_{min} slightly decreased during cycling of the poloxamer monolayers (data not shown).

By the addition of P188 into the subphase under the equilibrium DPoPE monolayer the dynamic characteristics of mixed DPoPE + P188 monolayers were studied. The γ decrease to the equilibrium value with time was monitored and then the mixed monolayers were cycled to 5-fold reduction of the initial area. Based on the results shown in Table 3 the γ_{max} values of the mixed DPoPE + P188 monolayers (at low P188 concentration) increased between the first and the second compression/decompression cycle in all cases, and were much higher for the lamellar L_α ($\Delta\gamma_{max}$ = 16.3 mN m^{-1}) in comparison with both non-lamellar phases ($\Delta\gamma_{max}$ = 8.1 mN m^{-1}). It should be noted that a hysteresis phenomenon was observed in all cases: the decompression curves of the mixed monolayers lied above the compression curves (data not shown), which could be both due to the "loss" of molecules from the surface (irreversible desorption) during compression and/or to the molecular rearrangement and reorganization at the surface of the mixed monolayers during cycling.

The different surface behavior of the lamellar phases compared to the non-lamellar ones at the low P188 concentration was much less pronounced according to the values of γ_{min} (Table 3). Moreover, the γ_{min} values at compression of all mixed DPoPE + P188 monolayes are similar to those of the pure DPoPE monolayers, thus confirming previous results indicating that at lower surface tensions (higher surface pressures) P188 is "squeezed out" from the films, leaving the lipid monolayers.[17,33]

Since not only molecular desorption but also molecular reorganization at the surface occurred during monolayer cycling it was informative (using the results in Table 3) to follow the change in γ_{max} between the 3rd and the 1st cycle ($\Delta\gamma_{max} = \gamma_{max}{}^3 - \gamma_{max}{}^1$) for

Table 3 Values of $\gamma_{max}/\gamma_{min}$ (mN m^{-1}) during 3 compression/decompression cycles of mixed DPoPE + P188 monolayers at different phase states. The experimental errors are ± 0.5 mN m^{-1} for the surface tension from three different measurements

Sample	No of cycle	Values of $\gamma_{max}/\gamma_{min}$ (mN m^{-1}): L_α phase γ_{eq} = 64.2	Q_{II} phase γ_{eq} = 67.3	H_{II} phase γ_{eq} = 68.6
DPoPE+low P188 concentration	1	51.8/26.2	60.6/30.3	56.2/27.1
	2	68.1/26.5	68.7/30.3	64.3/28.1
	3	66.8/27.5	67.8/29.3	63.7/28.1
DPoPE+middle P188 concentration	1	52.5/30.3	56.5/28.4	56.2/29.0
	2	59.3/31.8	59.3/26.5	61.5/30.0
	3	61.2/32.5	61.2/25.9	63.4/29.6
DPoPE+ high P188 concentration	1	52.5/29.2	53.1/31.5	50.6/28.4
	2	55.0/29.4	61.2/25.9	51.8/28.1
	3	61.5/29.6	60.3/26.2	52.5/28.5

each P188 concentration. Thus defined, we can assume qualitatively that higher $\Delta\gamma_{max}$ values reflect a bigger "loss" and/or desorption of molecules from the surface. The dependence between $\Delta\gamma_{max}$ of the mixed monolayers and the P188 concentration are illustrated in Fig. 4. It was shown that $\Delta\gamma_{max}$ for L_α and H_{II} phases increased with the decrease in P188 content (from group 3 to 1) in the monolayers (higher degree of desorption), while $\Delta\gamma_{max}$ values for Q_{II} phase remained practically the same at the different P188 concentrations. Based on these results we could speculate that the effects of desorption and reorganization in the monolayers during cycling are much more slightly pronounced in the Q_{II} phase. Thus we could suggest stronger interactions between P188 and DPoPE molecules in the Q_{II} phase than in the other two.

In addition, we followed the change in γ_{min} between the 1st and the 3rd cycle ($\Delta\gamma_{min} = \gamma_{min}{}^1 - \gamma_{min}{}^3$) for each P188 concentration (Table 3 and Fig. 5). As in Fig. 4, we observed quite different behavior for the Q_{II} phase as compared to L_α and H_{II} phases: only for the Q_{II} phase γ_{min} values diminished during cycling from the 1st to the 3rd cycle and accordingly $\Delta\gamma_{min}$ values increased from the 1st to the 3rd cycle for Q_{II} phase only (Fig. 5). In contrast to the increasing $\Delta\gamma_{max}$ values, the increase in $\Delta\gamma_{min}$

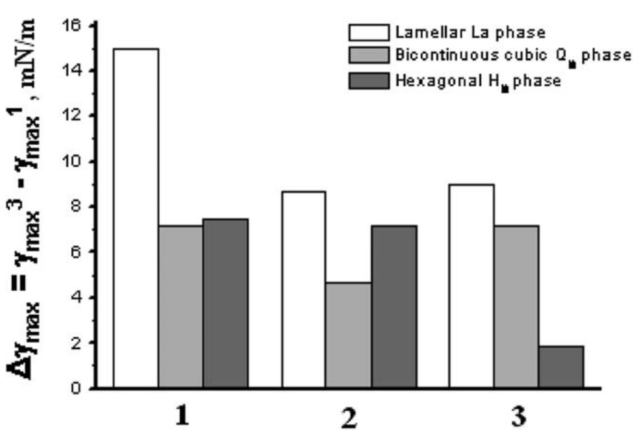

Fig. 4 Dependence of the P188 concentration on γ_{max} values between the 3rd and the 1st cycle ($\Delta\gamma_{max} = \gamma_{max}{}^3 - \gamma_{max}{}^1$) of mixed DPoPE + P188 monolayers on 0.5 M NaCl solution at 37 °C. Group 1 shows low P188 concentration (1 μg ml^{-1}), group 2 – middle P188 concentration (10 μg ml^{-1}) and group 3 - high P188 concentration (20 μg ml^{-1}).

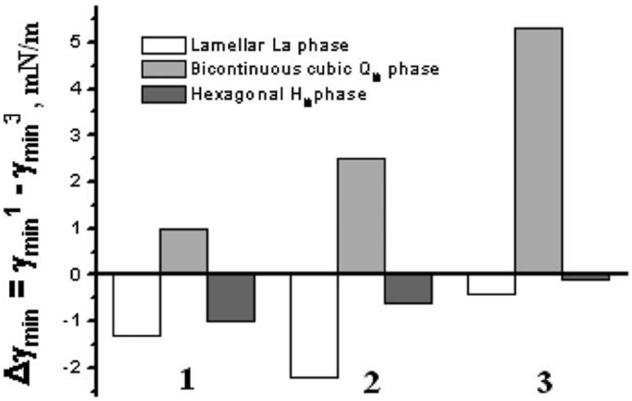

Fig. 5 Dependence of the P188 concentration on γ_{min} values between 1st and 3rd cycle ($\Delta\gamma_{min} = \gamma_{min}^1 - \gamma_{min}^3$) of mixed DPoPE + P188 monolayers on 0.5 M NaCl solution at 37 °C. Group 1 shows low P188 concentration (1 μg ml^{-1}), group 2 – middle P188 concentration (10 μg ml^{-1}) and group 3 - high P188 concentration (20 μg ml^{-1}).

during cycling showed a low degree of desorption, which had increased positive values for the monolayers of the cubic phase only (Fig. 5). The comparison between the lipid phases showed that the Q_{II} phase was characterized with the lowest degree of molecular desorption, *i.e.* with strongest interaction with P188 molecules (see Fig. 5 and Table 3).

Therefore, from the results above it was obvious that the lipid phase state had a strong influence on the behavior of the mixed films manifested by the dynamic characteristics of the mixed DPoPE + poloxamer monolayers during cycling. Moreover if we consider the change in γ_{min} values during cycling of the mixed monolayers in different DPoPE phases as a quantity of the rate of molecular desorption we could notice a completely opposite behavior of the mixed monolayers in the cubic phase in comparison with the other two.

Brewster angle microscopy of mixed P188 + DPoPE monolayers

Brewster angle microscopy (BAM) is a well established method for characterization of the morphology of ultrathin surface films on aqueous subphases. BAM images show contrast within the film resulted from differences in reflectivity of the p-polarized light incident at Brewster's angle from the monolayer as compared to the pure air–water interface.[49,50] Without a surface film the reflection is zero, but when the thin film forms the reflective index changes. This technique permits visualization of domains in the monolayer at low surface tension values.[53–55]

In this study we investigated the changes that occured at the spread DPoPE monolayers after the addition of P188 solution on the surface. The insoluble DPoPE monolayers were formed by spreading monomer phospholipid molecules dissolved in

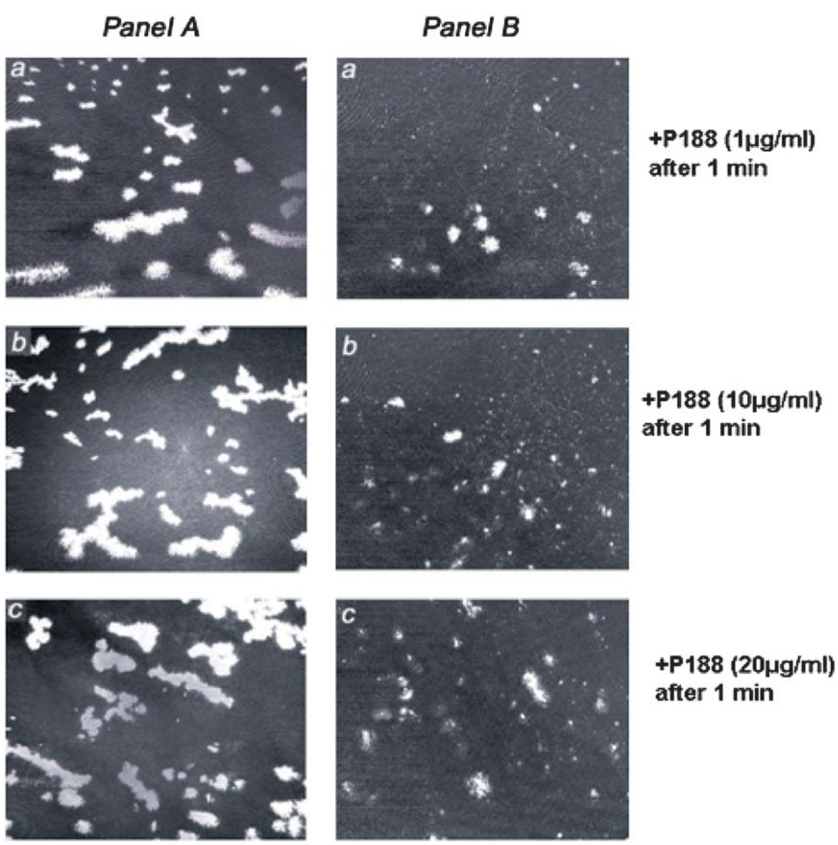

Fig. 6 BAM images of a pure DPoPE spread monolayer (with a surface concentration of 20 $Å^2$ per lipid molecule) over the subphase of 0.15 M NaC (Panel A) and BAM images of mixed DPoPE + P188 monolayers 1 min after the injection of a different volume concentration of P188 into the subphase of 0.15 M NaCl under previously formed DPoPE monolayer (Panel B). No effects of the increase in NaCl concentration on the surface lipid morphology were observed.

Table 4 Effects of the addition of Poloxamer 188 on the properties and stability of DPoPE films. $T = 22$ °C, pH = 7.0 In the concentration range 0.001–0.1 M NaCl C_t of DPoPE is 60 μg ml^{-1}, *i.e.* in these conditions the pure lipid thin liquid films are unstable and always rupture; t_1 is the film thinning time; τ is the film lifetime, see Experimental section. The final volume concentration of P188 is 86 μg ml^{-1}

		DPoPE films		DPoPE +P188 films	
DPoPE [μg ml^{-1}]	NaCl [M]	Film thinning time (t_1)	Film color and type	Film thinning time (t_1)	Film color and type
20	0.001	5 s	Thin to yellow, unstable (films always rupture)	4 min	Thin to gray, unstable (rupture after 4 min)
	0.01	20 s	Thin to yellow, unstable (films always rupture)	8 min	Thin to dark gray, unstable (rupture after 8 min)
	0.1	30 s	Thin to gray, unstable (films always rupture)	>8 min	Thin to dark gray, **stable** (τ > 15 min)
30	0.001	20 s	Thin to yellow, unstable (films always rupture)	4.5 min	Thin to gray, unstable (rupture after 4.5 min)
	0.01	25 s	Thin to gray, unstable (films always rupture)	9.5 min	Thin to dark gray, unstable (rupture after 9.5 min)
	0.1	30 s	Thin to gray, unstable (films always rupture)	> 9.5 min	Thin to dark gray, **stable** (τ > 15 min)
40	0.001	20 s	Thin to yellow, unstable (films always rupture)	3 min	Thin to dark gray, **stable** (τ > 15 min)
	0.01	20 s	Thin to gray, unstable (films always rupture)	3.5 min	Thin to dark gray, **stable** (τ > 15 min)
	0.1	30 s	Thin to gray, unstable (films always rupture)	4 min	Thin to dark gray, **stable** (τ > 15 min)
50	0.001	20 s	Thin to yellow, unstable (films always rupture)	4 min	Thin to dark gray, **stable** (τ > 15 min)
	0.01	25 s	Thin to gray, unstable (films always rupture)	4 min	Thin to dark gray, **stable** (τ > 15 min)
	0.1	40 s	Thin to dark gray, unstable (films always rupture)	4 min	Thin to dark gray, **stable** (τ > 15 min)

chloroform over 0.15 M NaCl subphase. At least 20 min were provided for chloroform evaporation. DPoPE was spread from chloroform solution, *i.e.* monomer lipid molecules, which resulted in better DPoPE spreading and lower equilibrium surface tension γ_{eq} values than in the case of DPoPE water dispersions (Fig. 1–3). The amount of DPoPE spread (at a surface concentration of 20 Å^2 per molecule) was enough to detect γ_{eq} of about 29 mN m^{-1} (data not shown) near to that of the native membranes. Therefore, the aim of our BAM experiments was to visualize the surface morphology of the pure DPoPE monolayers in comparison with the mixed DPoPE + poloxamer monolayers and to detect the size of the domains formed due to their interaction at the surface.

The BAM images of the pure DPoPE monolayer in the absence of P188 are shown in Fig. 6, panel A. Surface lipid structures with a different size, ranging from 20 to 150 μm were observed. One minute after the injection of increasing volume concentrations of the poloxamer (1, 10, and 20 μg ml^{-1}) into the subphase under a previously formed DPoPE monolayer a significant decrease in the domains size to 10–15 μm was observed (Fig. 6, panel B, images a to c). It should be noted that in all the proportions studied the effects of the interaction between DPoPE and P188 were practically the same; the BAM images obtained were similar and no visible dependence between the morphology of the surface structures and P188 concentration was observed. We could explain the decrease in the domains size with fast and strong poloxamer adsorption, and with its strong interactions with DPoPE molecules in the plane of the monolayer.

Effect of the addition of P188 on the properties and stability of DPoPE lipid thin liquid films (LTLFs)

In addition to the monolayer model system we examined the effect of the Poloxamer 188 on the morphology and stability of LTLFs, known in the literature also as foam films. The formation of both stable CBF and NBF is possible only at lipid concentration above the threshold concentration C_t (see Experimental section), since bellow C_t the films always rupture, *i.e.* the films are in unstable state. However, it was reported that in cases of long-chain polymers[37,38,56,57] the black films formed not by the above mentioned mechanism but by a continuous film thinning, without BS formation, until an equilibrium black films (so called, CBF-like) were obtained. It should be noted that we studied DPoPE films at known conditions (DPoPE and electrolyte concentrations) in which the film is unstable (below C_t), since we wanted to observe the effects of the addition of Poloxamer 188 to the *a priori* unstable DPoPE films.

By studying the evolution of the LTLF formation, observed by the film thinning time (t_1), type, color, and lifetime (τ), the effects of Poloxamer 188 were tested. The results are shown in Table 4. It was seen that pure DPoPE films at a concentration ranging from 20 to 50 μg ml^{-1} (in a different electrolyte concentration of NaCl) were unstable and always ruptured with increasing thinning time t_1 (between 5 and 40 s). The film color changed from yellow to dark-gray, indicating a decrease in the film thickness before DPoPE film rupture. The addition of P188 led in all cases to an increase in the film thinning time and stabilization of the mixed films. For example, at 30 μg ml^{-1} DPoPE in 0.1 M NaCl

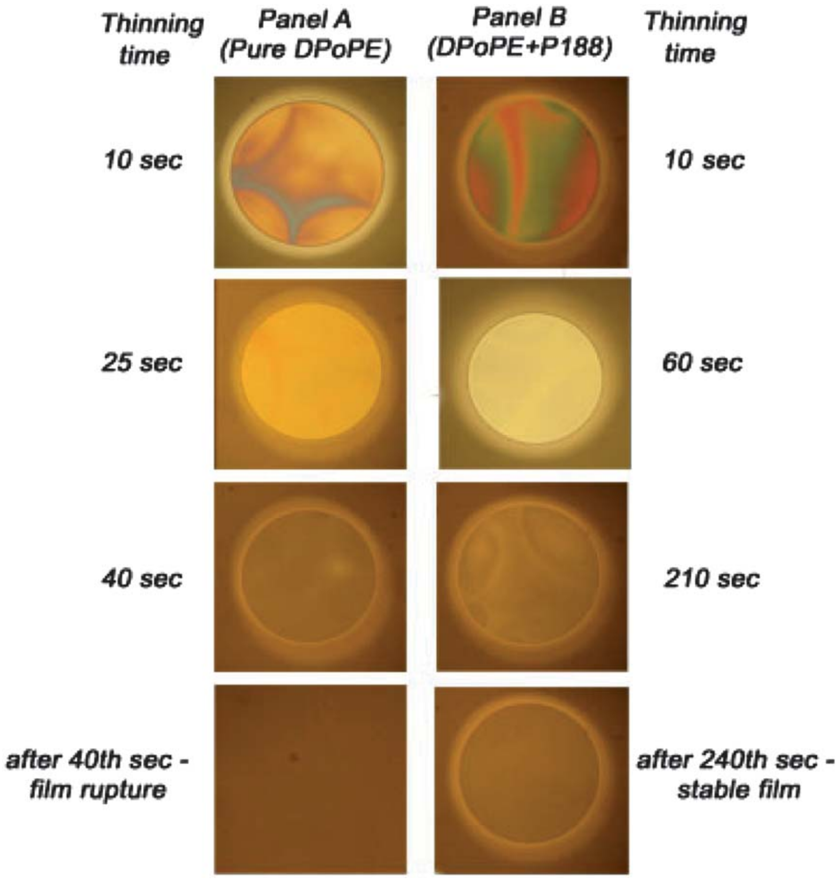

Fig. 7 Evolution of film thinning of pure DPoPE films (with concentration of 50 μg ml^{-1} in 0.1 M NaCl, Panel A) and after the addition of Poloxamer 188 to the drop of DPoPE (Panel B).

the films are unstable and rupture after $t_1 = 30$ s. However, in the presence of the poloxamer the thinning time increased to above 500 s until the formation of stable, dark-grey CBF-like films, and the film lifetime was more than 15 min. At higher DPoPE concentrations the same stabilization effect of P188 was observed (Table 4). It should be noted that the type of the mixed, stable DPoPE + P188 film was CBF-like, which had a thick free water layer between the monolayers. Even at very high electrolyte concentration (0.5 M NaCl) and DPoPE concentration above C_t, where pure DPoPE formed a much thinner NBF (without a free water layer between the monolayers, data not shown), the mixed DPoPE + P188 films were stable CBF-like. This allowed us to assume that, in addition to the stabilization effect, the presence of Poloxamer 188 provoked the appearance of an additional steric repulsion between the monolayers of the LTLFs, resulting in an increased thinning time and "disjoining" between the film monolayers leading to the formation of a thicker, dark grey, stable CBF-like film (Table 4, Fig. 7). The results, concerning the film stabilization effect of P188 are in agreement with previous studies.[37,38,56,57]

The differences in the hydrodynamic behavior between pure lipid films and mixed DPoPE + poloxamer films were also detected by a digital camera following the evolution of the film thinning (Fig. 7). It was found that DPoPE films at a concentration of 50 μg ml^{-1} always ruptured after 40 s, while the presence of Poloxamer 188 led to an increase in the thinning time and a formation of stable CBF-like films after 240 s with a lifetime of more than 15 min.

4. Conclusions

In this study, by using two model systems, lipid monolayer at the air–water interface and lipid thin liquid films the interaction between the Poloxamer 188 and DPoPE was investigated. The morphology and heterogeneity of the films surface was visualized by BAM. It should be noted that in the present work we used the term "interaction" in the context of molecular attractive/repulsive forces that arise between DPoPE and P188 molecules at the interface. Obviously these interactions influenced the properties, behavior, rate of desorption during compression, surface morphology, *etc.* of the mixed lipid/poloxamer films.

By the monolayer model system a different penetration degree of P188 to the lipid monolayers at a different lipid phase state (lamellar L_α and non-lamellar H_{II} and Q_{II}) was found for the first time. Regarding the rate and the degree of spreading of the different lipid phases at the interface the order $L_\alpha > Q_{II} > H_{II}$ was observed. It was shown that the penetration of P188 to the DPoPE monolayers in all three phases is very fast (within 20–30 s), strong and concentration dependent. The results revealed that the penetration of P188 at the low concentration used was stronger to the DPoPE monolayers in L_α and H_{II} phases in comparison to the Q_{II} phase. However, at high P188 concentration the strongest penetration was detected to the non-lamellar DPoPE monolayers in H_{II} and Q_{II} phases, followed by L_α phase.

The dynamic characteristics of the mixed DPoPE + P188 monolayers illustrated the effects of "loss" of molecules from the surface and desorption during monolayer compression–decompression, which are much better pronounced for the lamellar L_α phase in comparison to the non-lamellar H_{II} and Q_{II} phases. The results obtained suggested a stronger interaction between P188 and DPoPE during cycling of monolayers in the Q_{II} phase than in the other two and more packed structures formed at the surface in the case of the Q_{II} phase.

Hence, by the lipid monolayer experiments performed in this work on the penetration of poloxamer molecules to DPoPE monolayers in different phases (Fig. 1–3) and on the dynamic characteristics of the mixed monolayers (Fig. 4 and 5) it was clearly demonstrated that the lipid phase state strongly affected the behavior of the mixed films.

Our BAM experiments provided data on the surface morphology of the domains of the pure DPoPE monolayers spread from chloroform (at surface concentration at which γ_{eq} values are comparable with that of the native membranes) and after the addition of the poloxamer to the monolayers. The results obtained allowed to detect the changes in the size of the domains formed due to the interaction between P188 and DPoPE at the surface. These experiments showed that the addition of P188 to DPoPE monolayers led to a decrease in the lipid domain size and to formation of more homogeneous films.

It was shown qualitatively by LTLFs for the first time, a strong stabilization effect of Poloxamer 188 to the *a priori* unstable DPoPE films, probably influenced by the appearance of steric repulsion (in addition to the electrostatic repulsion and van der Waals attractive forces) between the lipid monolayers of LTLF (*i.e.* appearance of steric component of the disjoining pressure), due to the presence of the amphiphilic polymer molecules in the water core between them.

On the basis of the results obtained we can conclude that the three-block copolymer Poloxamer 188 possesses strong affinity to phospholipid molecules located at the membrane surface. The results suggested that the non-lamellar H_{II} and Q_{II} lipid phases have a higher potential to act as a "reservoir" for penetrating agents, and as a pool for membrane repairing substances, like P188. Both qualitative and quantitative results obtained could be of importance in clarifying the mechanisms of effective sealing of the local damaged cell membranes by Poloxamer 188 molecules. Our investigations in this direction are in progress.

Acknowledgements

This research was supported by The Scientific Foundation of the Bulgarian Ministry of Education and Science (grants N DO 02 – 107/08 and DRG 02/5).

References

1 P. Cullis and B. De Kruijff, *Biochim. Biophys. Acta*, 1979, **559**, 399.
2 D. Siegel, *Biophys. J.*, 1993, **65**, 2124.
3 D. Siegel, *Biophys. J.*, 1986, **49**, 1171.
4 Z. Lalchev, in *Surface Properties of Lipids and Proteins at Bio-Interfaces, Handbook of Surface and Colloid Chemistry*, ed. K. S. Birdi, CRC Press, Boca Raton–New York–London–Tokyo, 1997, p. 625.
5 M. Wikstrom, J. Xie, M. Bogdanov, E. Mileykovskaya, P. Heacock, A. Wieslander and W. Dowhan, *J. Biol. Chem.*, 2003, **279**, 10484.
6 J. Jensen and J. Schutzbach, *Biochemistry*, 1984, **23**, 1115.
7 J. Seddon and R. Templer, in *Handbook of Biological Physics*, ed. R. Lipowsky and E. Sackmann, Elsevier Science B.V., 1995, p. 97.
8 J. M. Seddon, *Biochim. Biophys. Acta*, 1990, **1031**, 1.
9 P. R. Cullis M. J. Hope, B. DeKruijff, A. J. Verkleij, C. P. S. Tilcock, in *Phospholipids and cellular regulation*, ed. J. F. Kuo, CRC Press, Boca Raton, 1985, p. 1.
10 Y. Nishizuka, *Nature*, 1984, **308**, 693.
11 D. C. Litzinger and L. Huang, *Biochim. Biophys. Acta*, 1992, **1113**, 201.
12 R. C. Lee, L. P. River, F.-S. Pan, L. Ji and R. L. Wollmann, *Proc. Natl. Acad. Sci. U. S. A.*, 1992, **89**, 4524.
13 D. Kilinc, G. Gallo and K. A. Barbee, *Exp. Neurol.*, 2008, **212**, 422.
14 B. I. Tropea and R. C. Lee, *J. Biomech. Eng.*, 1992, **114**, 241.
15 V. Sharma and K. Stebe, *Biophys. J.*, 1996, **71**, 3229.
16 A. D. Murphy, M. C. McCormack, D. Bichara, M. A. Randolph and W. G. AustenJr., *J. Surg. Res.*, 2009, **151**, 220.
17 S. A. Maskarinec and J. Hannig, *Biophys. J.*, 2002, **82**, 1453.
18 R. C. Lee, A. Myerov and C. P. Maloney, *Ann. N. Y. Acad. Sci.*, 1994, **720**, 239.
19 G. Wu, J. Majewski, C. Ege, K. Kjaer, M. J. Weygand and Ka Yee C. Lee, *Biophys. J.*, 2005, **89**, 3159.
20 J. Hanning, D. Zhang and D. J. Canaday, *Radiat. Res.*, 2000, **154**, 171.
21 F. A. Merchant and W. H. Holmes, *J. Surg. Res.*, 1998, **74**, 131.
22 S. Bajaj, T. Shoemaker, A. Hakimiyan, L. Rappoport, C. Pascual-Garrido, T. R. Oegema, M. A. Wimmer and S. Chubinskaya, *J. Orthop. Trauma*, 2010, **24**, 571.
23 Jia-Yu Wang, J. Chin, J. Marks and C. Lee Ka Yee, *Biophys. J.*, 2009, **96**, 164a.
24 J. T. Padanilam, J. C. Bischof and R. C. Lee, *Ann. N. Y. Acad. Sci.*, 1994, **720**, 111.
25 F. A. Merchant, W. H. Holmes, M. Capelli-Schellpfeffer, R. C. Lee and M. Toner, *J. Surg. Res.*, 1998, **74**, 131.
26 B. Greenebaum, C. S. Carrillo, J. Hannig, M. A. Beckett, R. R. Weichselbaum and R. C. Lee, *Burns*, 2004, **30**, 539.
27 S. Yasuda, D. Townsend, D. E. Michele, E. G. Favre, S. M. Day and J. M. Metzger, *Nature*, 2005, **436**, 1025.
28 J. T. Nguyen, M. A. Medina, M. C. McCormack, M. A. Randolph and W. G. Austen Jr., *J. Surg. Res.*, 2009, **151**, 210.
29 D. Frim, D. A. Wright, D. J. Curry, W. Cromie, R. Lee and Un Jung Kang, *Cognitive neurosci. neuropsych.*, 2004, **15**, 171.
30 S. Gelperina, O. Maksimenko, A. Khalansky, L. Vanchugova, E. Shipulo, K. ABiochim. Biophys. Actasova, R. Berdiev, S. Wohlfart, N. Chepurnova and J. Kreuter, *Eur. J. Pharm. Biopharm.*, 2010, **74**, 157.
31 Y. Zhang, L. Tang, L. Sun, J. Bao, C. Song, L. Huang, K. Liu, Y. Tian, Ge Tian, Z. Li, H. Sun and L. Mei, *Acta Biomater.*, 2010, **6**, 2045.
32 G. Wu and Ka Yee C. Lee, *Langmuir*, 2009, **25**, 2133.
33 C. Weingarten, N. S. S. Magalhaes, A. Baszkin, S. Benita and M. Seiller, *Int. J. Pharm.*, 1991, **75**, 171.
34 A. Jordanova, Z. Lalchev and B. Tenchov, *Eur. Biophys. J.*, 2003, **31**, 626.
35 A. Jordanova, B. Tenchov and Z. Lalchev, *Annuare de l'Universite de Sofia*, 2004, **96**, 33.
36 Z. Lalchev, in T. Tadros (Ed.) *Colloid Stability – The role of Surface Forces*, Wiley-VCH Verlag GmbH, 2006, 383.
37 G. As. Georgiev, G. D. Georgiev and Z. Lalchev, *Eur. Biophys. J.*, 2006, **35**, 352.
38 G. Georgiev and Z. Lalchev, *Eur. Biophys. J.*, 2004, **33**, 742.
39 S. Naydenova, Z. Lalchev, A. Petrov and D. Exerowa, *Eur. Biophys. J.*, 1990, **17**, 343.
40 D. Exerowa, Z. Lalchev, B. Marinov and K. Ognyanov, *Langmuir*, 1986, **2**, 664.
41 D. Exerowa and Z. Lalchev, *Langmuir*, 1986, **2**, 668.
42 Z. Lalchev, G. Georgiev, A. Jordanova, R. Todorov, E. Christova and C. Vassilieff, *Colloids Surf., B*, 2004, **33**, 227.
43 E. Scarpelli, A. Mautone, Z. Lalchev and D. Exerowa, *Colloids Surf., B*, 1997, **8**, 133.

44 R. Cohen, R. Todorov, S. Alexandrov, Y. Christova, Z. Lalchev and D. Exerowa, *Colloids Polym Sci.*, 2005, **284**, 546.
45 B. A. Hills, *The biology of surfactant, Cambridge*: Cambridge University Press, 1988.
46 I. Panaiotov, T. Ivanova, K. Balashev and J. Proust, *Colloids Surf., A*, 1995, **102**, 159.
47 V. Raneva, M. Ivanova, Tz. Ivanova, E. Rogalska, R. Verger and I. Panaiotov, *Colloids Surf., B*, 1995, **4**, 213.
48 B. Tenchov, R. Koynova and G. Rapp, *Biophys. J.*, 1998, **75**, 853.
49 S. Henon and J. Meunier, *Rev. Sci. Instrum.*, 1991, **62**, 936.
50 D. Honing and D. Mobius, *J. Phys. Chem.*, 1991, **95**, 4590.
51 A. Sheludko, *Adv. Colloid Interface Sci.*, 1967, **1**, 391.
52 D. Exerowa and P. M. Kruglyakov, *Foam and Foam Films-Theory, Experiment, Application*, Elsevier, Amsterdam, 1998.
53 F. Wu, A. Gericke, C. Flash, T. Mealy, B. Seaton and R. Mendelsohn, *Biophys. J.*, 1998, **74**, 3273.
54 J. Saccani, S. Castano, B. Desbat and D. Blauder, *Biophys. J.*, 2003, **85**, 3781.
55 K. Winsel, D. Honing, K. Lunkenheimer, K. Geggel and C. Witt, *Eur. Biophys. J.*, 2003, **32**, 544.
56 R. Sedev, D. Exerowa and G. H. Findenegg, *Colloid Polym. Sci.*, 2000, **278**, 119.
57 R. Sedev and D. Exerowa, *Adv. Colloid Interface Sci.*, 1999, **83**, 111.